Acta Cryst. (1971). A27, 332

Determination of the Polarization Vectors of Lattice Waves by Anomalous Neutron Scattering

BY T. G. RAMESH AND S. RAMASESHAN

Materials Science Division, National Aeronautical Laboratory, Bangalore-17, India

(*Received* 24 *August* 1970)

The Argand diagram representation of coherent inelastic scattering (one-phonon process) is presented. This is used to show that $|F(\mathbf{H},\mathbf{q})| \neq |F(\tilde{\mathbf{H}},\tilde{\mathbf{q}})|$ in a non-centrosymmetric two-atom structure when an anomalous scatterer is present and $|F(\mathbf{H},\mathbf{q})| \neq |F(\mathbf{H},\tilde{\mathbf{q}})|$ even in a NaCl-type structure when both atoms are normal scatterers. This paper describes how the polarization vectors of lattice waves may be experimentally determined in a crystal containing a nuclide which scatters thermal neutrons anomalously. The procedures for the determination of the polarization vectors in centrosymmetric and non-centrosymmetric structures when they are, in general, complex and for a Bravais lattice when they are always linearly polarized have also been presented. It is shown that the 'phase problem' associated with the determination of the initial phase of elliptic motion can, in principle, be solved by using anomalous neutron scattering.

1. Introduction

The importance of experimentally determining the polarization vectors of lattice waves has been recognized by many authors (Brockhouse, 1964; Dolling & Woods, 1965). Unlike the eigenvalues of the dynamical matrix, the components of the polarization vector are always linear functions of the elements of the dynamical matrix. Thus the determination of the interatomic force constants through the measured frequencies and the polarization vectors, provides an advantage over the method of non-linear fitting of the dynamical equation to the observed frequencies. In some specially simple cases when $\mathbf{q}$, the wave-vector of the lattice wave lies in a symmetry plane or is along a symmetry axis, the direction of the polarization vector may be determined from symmetry considerations. This is probably the reason why most of the experiments on inelastic scattering are confined to wave propagation along a symmetry direction. We shall concern ourselves with wave propagation along a general direction in the crystal and attempt to obtain the components of the polarization vector from the observed intensity data. Recently Cochran (1968) suggested the method of inelastic Patterson synthesis to extract information about the polarization vectors and discussed the inherent difficulties involved in interpreting this synthesis. Only at $\mathbf{q}=0$, has the synthesis a simple interpretation. Further, this method requires the collection of the intensity data of the coherent one-phonon scattering near a large number of reciprocal-lattice points and thus poses a number of experimental problems. Ramaseshan & Viswanathan (1970) showed that the breakdown of Friedel's law in inelastic scattering, in a crystal which has at least one anomalous scatterer can yield information regarding the polarization vectors of lattice waves. In this paper, the relevant experimental data to be collected and the mode of extracting the components of the polarization vector are discussed. Further, the Argand diagram representation of the coherent one-phonon process in the presence and absence of anomalous neutron scattering is presented. This representation simplifies the writing down of the structure factors in complex structures and helps in visualizing the differences in structure factors under various experimental conditions.

2. Anomalous neutron scattering

Peterson & Smith (1961, 1962) showed that thermal neutrons are scattered anomalously by some nuclides like Cd^{113}, Sm^{149}, Eu^{151} and Gd^{157} leading to the violation of Friedel's law in non-centrosymmetric structures. The anomalous neutron scattering length of an atom B has the form

$$b_B = b_{B_0} + b'_B + ib''_B \qquad (1)$$

where b_{B_0} represents the normal scattering length while b'_B and b''_B correspond to dispersion terms. A typical dispersion curve of b' and b'' for Cd^{113} is given in Fig. 1. b''_B is always positive whereas b'_B may take both positive and negative values, a behaviour markedly different from that in X-ray scattering. In the Figures that illustrate this paper, b'_B has been taken as positive.

Ramaseshan (1966) pointed out that since $b'_B/b_{B_0} \simeq 4{\cdot}0$–$5{\cdot}0$ and $b''_B/b_{B_0} \simeq 8$, almost two orders of magnitude larger than the corresponding quantities in X-ray scattering, anomalous neutron scattering may well be used to solve large structures provided accurate measurements of the intensity is possible. The method of doing this was worked out by Singh & Ramaseshan (1968). These techniques used in structural crystallography may be directly applied to yield the components of the polarization vector, since the coherent inelastic scattering results from the interference of wavelets from a crystal the equilibrium configuration of which is perturbed by a propagating lattice wave.

3. Description of the polarization vector and coherent one-phonon process

For the discussion that follows, it is necessary to describe briefly the polarization vector and its relationship to the coherent one-phonon process. We follow the general notation used by Maradudin, Montroll & Weiss (1963). Consider a crystal with a unit cell having r atoms. The position vector of the κth atom in the lth unit cell is given by

$$\mathbf{x}(l_\kappa)=\mathbf{x}(l)+\mathbf{x}(\kappa)$$

$\mathbf{x}(l)$ defines the origin of the lth unit cell relative to some origin in the crystal and $\mathbf{x}(\kappa)$ defines the position of the κth atom relative to the cell origin. We shall confine ourselves to the 'harmonic approximation'. Then the equation of motion of the crystal is given by

$$M_\kappa \ddot{u}_\alpha(l\kappa)=-\sum_{l'\kappa'\beta}\Phi_{\alpha\beta}(l\kappa;\, l'\kappa')\, u_\beta(l'\kappa')$$

where $\alpha,\beta=1,2,3$ correspond to the three cartesian components and $\mathbf{u}(l\kappa)$ denotes the displacement of the κth atom in the lth cell from the equilibrium configuration. We seek a solution where the displacements are of the form

$$\mathbf{u}(l\kappa)=\sum_{\mathbf{q}j}\frac{\mathbf{u}_{\mathbf{q}j}(0)}{\sqrt{M_\kappa}}\,\mathbf{e}(\kappa|_j^{\mathbf{q}})\,\exp i\{\mathbf{q}\,.\,\mathbf{x}(l_\kappa)-\omega_j(\mathbf{q})t\}\,.$$

$u_{\mathbf{q}j}(0)$ represents the scalar amplitude, directly related to the energy of the mode in thermal equilibrium, and does not enter the dynamical equation. $\mathbf{e}(\kappa|_j^{\mathbf{q}})$ denotes the eigenvector of the κth atom for the mode $(_j^{\mathbf{q}})$. Thus, the equations of motion could be written as

$$\omega_j^2(\mathbf{q})\, e_\alpha(\kappa|_j^{\mathbf{q}})=-\sum_{\kappa'\beta}D_{\alpha\beta}(\kappa\kappa'|\mathbf{q})\, e_\beta(\kappa'|_j^{\mathbf{q}}),$$
$$j=1,2,\ldots 3r;\ \alpha,\beta=1,2,3\,.$$

$D_{\alpha\beta}(\kappa\kappa'|\mathbf{q})$ are the elements of the 'dynamical matrix' which are related to the inter-atomic force constants $\Phi_{\alpha\beta}(0\kappa;\, l'-l\kappa')$ through the relation,

$$\Phi_{\alpha\beta}(0\kappa;\, l'-l\kappa')=\sqrt{M_\kappa M_{\kappa'}}\sum_{\mathbf{q}}D_{\alpha\beta}(\kappa\kappa'|\mathbf{q})\times\exp -i\{\mathbf{q}\,.\,\mathbf{x}(_{\kappa'}^{l'-l})-\mathbf{x}(_\kappa^l)\}\,.$$

The coefficients $e_\alpha(\kappa|_j^{\mathbf{q}})$ for a given $\mathbf{q}$ and j and for different atoms in the unit cell are regarded as the components of a $3r$ dimensional vector of unit magnitude called the 'polarization vector'. The enumeration of these coefficients gives us the relative amplitudes of the different atoms in the unit cell.

The eigenvectors satisfy the orthonormality condition

$$\sum_{\kappa\alpha}e_\alpha^*(\kappa|_j^{\mathbf{q}})\, e_\alpha(\kappa|_{j'}^{\mathbf{q}})=\delta_{jj'}\,. \qquad (6)$$

Since the elements of the dynamical matrix are complex quantities, the eigenvectors are in general complex. Only when each atom in the structure lies at a centre of inversion, the dynamical matrix could be transformed into a real symmetric matrix, and the corresponding eigenvectors would be real. The significance of the eigenvectors being complex is that the motion

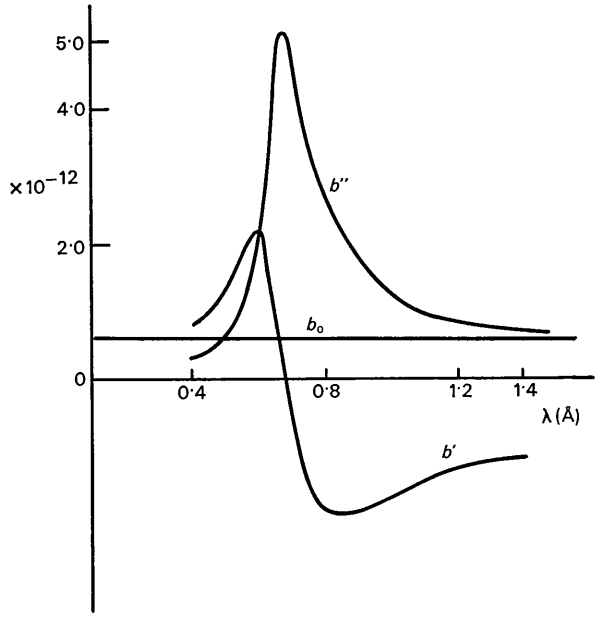

Fig. 1. Variation of b' and b'' with wavelength for Cd^{113}

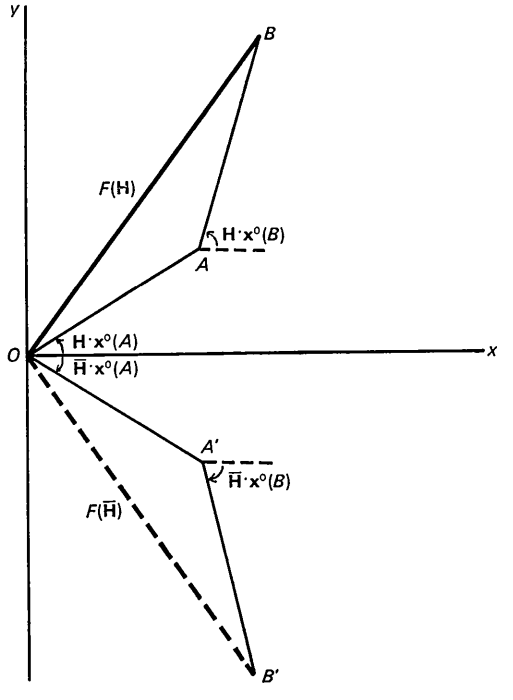

Fig. 2. Bragg reflexion – two atom structure; normal scattering. $OA=OA'=b_A\exp\{-W_A\}$, $AB=A'B'=b_B\exp\{-W_B\}$; $|F(\mathbf{H})|=|F(\bar{\mathbf{H}})|$.

of an atom under the influence of a lattice wave is elliptic.

We write $\mathbf{e}(\kappa|_j^{\mathbf{q}}) = \mathbf{A} + i\mathbf{B}$ (7)

$$\text{where } \mathbf{A} = \begin{bmatrix} a_1 \\ a_2 \\ a_3 \end{bmatrix} \text{ and } \mathbf{B} = \begin{bmatrix} b_1 \\ b_2 \\ b_3 \end{bmatrix}.$$

Thus the six components of the real vectors **A** and **B** specify the elliptic motion of a given atom. In a two atom structure and for **q** in a general direction, we require twelve components to describe completely the elliptic motions of the two atoms. At $\mathbf{q}=0$, for all structures, the elliptic motion degenerates into a linear one and the initial phase of motion will be either 0 or π. The phase difference between the two atoms is 0 for the acoustic mode and π for the optical mode.

The differential cross section for one-phenon scattering, with the usual notion, is given by

$$\frac{\mathrm{d}^2\sigma}{\mathrm{d}\Omega \mathrm{d}\varepsilon} = \frac{k}{\hbar k_0} S(\mathbf{K}, \omega)$$

where

$$S(\mathbf{K},\omega) = \frac{N\hbar\{\bar{n}(\mathbf{q}_j) + \tfrac{1}{2} \mp \tfrac{1}{2}\}}{4\pi\omega_j(\mathbf{q})}$$

$$\times \left| \frac{b_A}{\sqrt{M_A}} \exp\{-W_A\}\mathbf{K} \cdot \mathbf{e}(A|_j^{\mathbf{q}}) \exp\{i\mathbf{H} \cdot \mathbf{x}^0(A)\} \right.$$

$$\left. + \frac{b_B}{\sqrt{M_B}} \exp\{-W_B\}\mathbf{K} \cdot \mathbf{e}(B|_j^{\mathbf{q}}) \exp\{i\mathbf{H} \cdot \mathbf{x}^0(B)\} \right|^2$$

$$\times \delta[\omega \mp \omega_j(\mathbf{q})]\, \delta[\mathbf{K} \mp \mathbf{q} - \mathbf{H}]. \quad (8)$$

$\mathbf{x}^0(A)$ and $\mathbf{x}^0(B)$ represent the equilibrium position vectors of the two atoms A and B in the unit cell. b_A and b_B denote the coherent scattering lengths of the two nuclei respectively. The positive sign represents the phonon creation process whereas the negative sign represents the annihilation process. The two δ functions represent the conservation of energy and crystal momentum during the scattering process. $\mathbf{K} = \mathbf{k} - \mathbf{k}_0$ is the scattering vector or the momentum transfer vector. **H** is a reciprocal-lattice vector. The scattering vector $\bar{\mathbf{K}}$ associated with $\bar{\mathbf{H}}$ satisfies the momentum conservation law

$$\bar{\mathbf{K}} = \bar{\mathbf{H}} + \bar{\mathbf{q}}. \quad (8a)$$

From equation (8) it is clear that we can define an inelastic structure factor, $F(\mathbf{K})$, given by

$$F(\mathbf{K}) = \frac{b_A}{\sqrt{M_A}} \exp\{-W_A\}\mathbf{K} \cdot \mathbf{e}(A|_j^{\mathbf{q}}) \exp\{i\mathbf{H} \cdot \mathbf{x}^0(A)\}$$

$$+ \frac{b_B}{\sqrt{M_B}} \exp\{-W_B\}\mathbf{K} \cdot \mathbf{e}(B|_j^{\mathbf{q}}) \exp\{i\mathbf{H} \cdot \mathbf{x}^0(B)\}.$$

Thus $\mathbf{K} \cdot \mathbf{e}(A|_j^{\mathbf{q}})$ and $\mathbf{K} \cdot \mathbf{e}(B|_j^{\mathbf{q}})$ represent the probability amplitudes for one-phonon scattering so that $(b_A/\sqrt{M_A}) \exp\{-W_A\}\mathbf{K} \cdot \mathbf{e}(A|_j^{\mathbf{q}})$ and $(b_B/\sqrt{M_B}) \times \exp\{-W_B\}\mathbf{K} \cdot \mathbf{e}(B|_j^{\mathbf{q}})$ may be considered as the scattering lengths of the two atoms for the coherent one-phonon scattering.

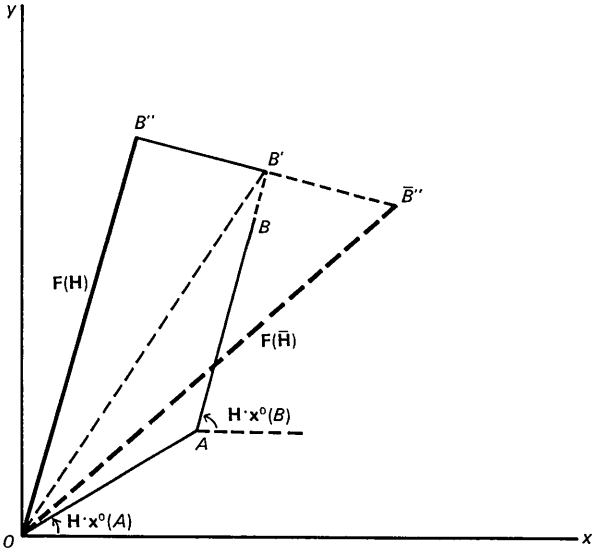

Fig. 3. Bragg reflexion – two atom structure with atom B, an anomalous scatterer. $OA = b_A \exp\{-W_A\}$, $AB = b_{B_0} \times \exp\{-W_B\}$, $BB' = b'_B \exp\{-W_B\}$ and $B'B'' = b''_B \times \exp\{-W_B\}$; $|F(\mathbf{H})| \neq |F(\bar{\mathbf{H}})|$.

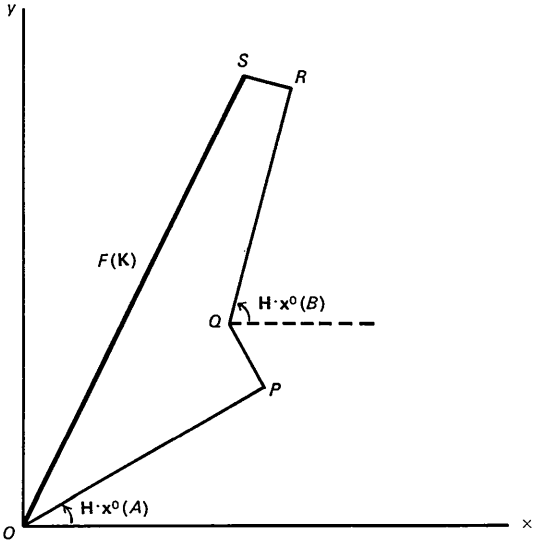

Fig. 4. One-phonon scattering in a non-centrosymmetric structure; normal scattering.

$$OP = \frac{b_A}{\sqrt{M_A}} \exp\{-W_A\}\mathbf{K} \cdot \mathbf{P},$$

$$PQ = \frac{b_A}{\sqrt{M_A}} \exp\{-W_A\}\mathbf{K} \cdot \mathbf{Q},$$

$$QR = \frac{b_B}{\sqrt{M_B}} \exp\{-W_B\}\mathbf{K} \cdot \mathbf{R}$$

and $RS = \frac{b_B}{\sqrt{M_B}} \exp\{-W_B\}\mathbf{K} \cdot \mathbf{S}$; $|F(\mathbf{K})| = |F(\bar{\mathbf{K}})|$.

4. Argand diagram representation: non-centrosymmetric structures

(a) Bragg reflexion: normal and anomalous scattering

Fig. 2 gives the Argand diagram for a Bragg reflexion in a non-centrosymmetric structure containing two atoms per unit cell, both being normal scatterers for neutrons. The reciprocal-lattice vectors $\mathbf{H}$ and $\bar{\mathbf{H}}$ represent the reflexions from the planes (hkl) and $(\bar{h}\bar{k}\bar{l})$ respectively. In Fig. 2

$$OA = b_A \exp\{-W_A\} \text{ and } AB = b_B \exp\{-W_B\}$$

where b_A and b_B are the normal scattering lengths of the two atoms. $\exp\{-W_A\}$ and $\exp\{-W_B\}$ are the Debye–Waller factors for the two atoms. In X-ray crystallographic practice, it is the convention to reflect the Argand diagram of $F(\bar{\mathbf{H}})$ about the real axis to facilitate the comparison of $F(\mathbf{H})$ and $F(\bar{\mathbf{H}})$. We shall follow this convention in this paper. From Fig. 2, it is clear that $|F(\mathbf{H})| = |F(\bar{\mathbf{H}})|$, leading to Friedel's law. Fig. 3 represents the situation when the atom B in the structure becomes an anomalous scatterer for thermal neutrons. The scattering length of atom B is given by equation (1). In Fig. 3, $BB' = b'_B \exp\{-W_B\}$ and $B'B'' =$

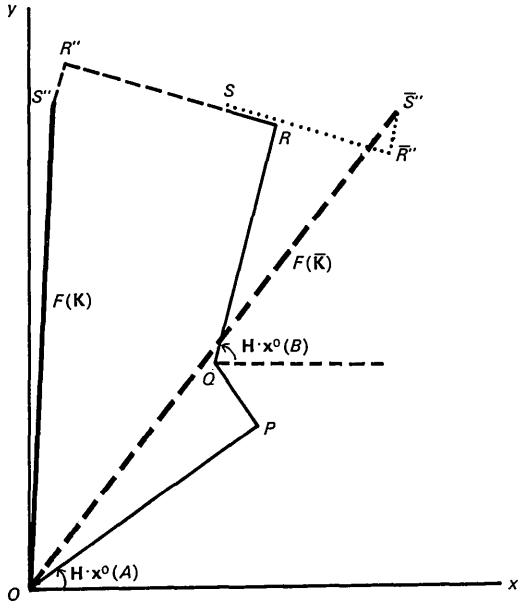

Fig. 5. One-phonon scattering – atom B, an anomalous scatterer.

$$QR = \frac{(b_{B_0} + b'_B)}{\sqrt{M_B}} \exp\{-W_B\}\,\mathbf{K}\,.\,\mathbf{R},$$

$$RS = \frac{(b_{B_0} + b'_B)}{\sqrt{M_B}} \exp\{-W_B\}\mathbf{K}\,.\,\mathbf{S},$$

$$SR'' = S\bar{R}'' = \frac{b''_B}{\sqrt{M_B}} \exp\{-W_B\}\mathbf{K}\,.\,\mathbf{R}$$

and $$R''S'' = \bar{R}''\bar{S}'' = \frac{b''_B}{\sqrt{M_B}} \exp\{-W_B\}\mathbf{K}\,.\,\mathbf{S};$$

$$|F(\mathbf{K})| \neq |F(\bar{\mathbf{K}})|.$$

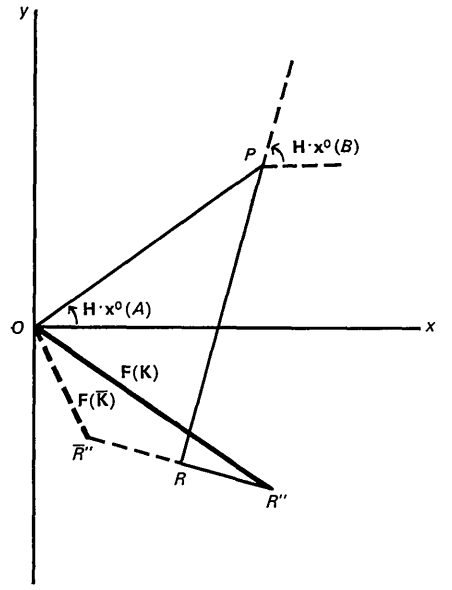

Fig. 6. Interaction with an optical phonon – atom B, an anomalous scatterer.

$$OP = \frac{b_A}{\sqrt{M_A}} \exp\{-W_A\}\mathbf{K}\,.\,\mathbf{P},$$

$$PR = \frac{(b_{B_0} + b'_B)}{\sqrt{M_B}} \exp\{-W_B\}\,\mathbf{K}\,.\,\mathbf{R},$$

$$RR'' = R\bar{R}'' = \frac{b''_B}{\sqrt{M_B}} \exp\{-W_B\}\mathbf{K}\,.\,\mathbf{R};$$

$$|F(\mathbf{K})| \neq |F(\bar{\mathbf{K}})|.$$

$b''_B \exp\{-W_B\}$. Since the relative phase of $(b_{B_0} + b'_B)$ and b''_B is independent of the scattering vectors $\mathbf{H}$ and $\bar{\mathbf{H}}$, we get $|F(\mathbf{H})| \neq |F(\bar{\mathbf{H}})|$ leading to the breakdown of Friedel's law.

(b) Coherent one-phonon process: normal scattering

For a general $\mathbf{q}$, the two atoms in the unit cell describe elliptic motions. We write the eigenvectors of the two atoms as

$$\left.\begin{aligned} \mathbf{e}(A|_j^{\mathbf{q}}) &= \mathbf{P} + i\mathbf{Q} \\ \text{and} \qquad \mathbf{e}(B|_j^{\mathbf{q}}) &= \mathbf{R} + i\mathbf{S}\,. \end{aligned}\right\} \tag{9}$$

$$\mathbf{P} = \begin{bmatrix} p_1 \\ p_2 \\ p_3 \end{bmatrix}, \quad \mathbf{Q} = \begin{bmatrix} q_1 \\ q_2 \\ q_3 \end{bmatrix}, \quad \mathbf{R} = \begin{bmatrix} r_1 \\ r_2 \\ r_3 \end{bmatrix} \text{ and } \mathbf{S} = \begin{bmatrix} s_1 \\ s_2 \\ s_3 \end{bmatrix}.$$

P, **Q**, **R** and **S** are real vectors and thus twelve components are required to describe completely their elliptic motions. The polarization vector, $\mathbf{V}(_j^{\mathbf{q}})$, which is normalized to unit magnitude is a column matrix given by

$$\mathbf{V}(_j^{\mathbf{q}}) = \begin{bmatrix} p_1 + iq_1 \\ p_2 + iq_2 \\ p_3 + iq_3 \\ r_1 + is_1 \\ r_2 + is_2 \\ r_3 + is_3 \end{bmatrix}.$$

The complete enumeration of these twelve components gives us the relative amplitudes and phases of the two atoms in the unit cell. The initial phase of the elliptic motion is determined by the magnitude of the interatomic forces and hence cannot be determined by symmetry considerations. From equation (9), we get

$$\mathbf{K}\,.\,\mathbf{e}(A|_j^{\mathbf{q}})=\mathbf{K}\,.\,\mathbf{P}+\exp\{i\pi/2\}\,\mathbf{K}\,.\,\mathbf{Q}$$
$$\text{and } \mathbf{K}\,.\,\mathbf{e}(B|_j^{\mathbf{q}})=\mathbf{K}\,.\,\mathbf{R}+\exp\{i\pi/2\}\,\mathbf{K}\,.\,\mathbf{S}\,. \qquad (10)$$

Fig. 4. represents the Argand diagram for one-phonon scattering. $F(\mathbf{K})$ represents the structure factor for coherent one-phonon process corresponding to the point defined by $\mathbf{K}$ on the 'scattering surface'. From the relation (8*a*), it is clear that the point defined by $\bar{\mathbf{K}}$ on the scattering surface is associated with the lattice wave of wave-vector $\bar{\mathbf{q}}$. For $\bar{\mathbf{q}}$, the eigenvectors of the two atoms are complex conjugates of the corresponding quantities for $\mathbf{q}$, signifying that the sense of description of the ellipse will now be in the opposite direction. That is

$$\left.\begin{aligned}\mathbf{e}(A|_j^{\bar{\mathbf{q}}})&=\mathbf{P}-i\mathbf{Q}\\ \text{and}\quad \mathbf{e}(B|_j^{\bar{\mathbf{q}}})&=\mathbf{R}-i\mathbf{S}\,.\end{aligned}\right\} \qquad (11)$$

Thus the structure factor for $\bar{\mathbf{K}}$ is the complex conjugate of that for $\mathbf{K}$ so that the intensity is equal at these two points on the scattering surface.

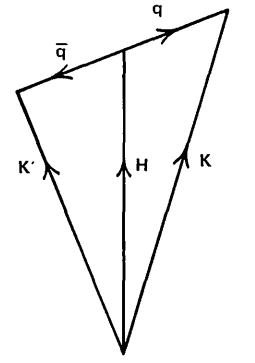

(*a*)

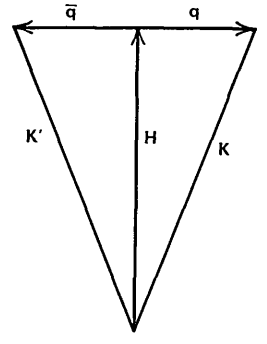

(*b*)

Fig. 7. Schematic diagram of the momentum conservation law (*a*) general case $|\mathbf{K}|\neq|\mathbf{K}'|$, (*b*) special case $|\mathbf{K}|=|\mathbf{K}'|$.

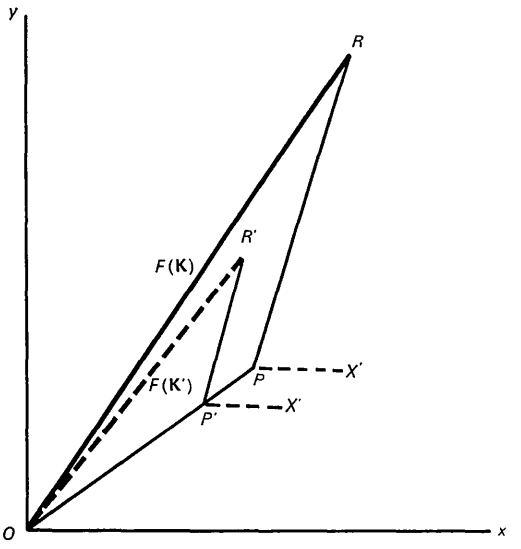

Fig. 8. One-phonon absorption and emission processes near a reciprocal-lattice point – eigenvectors real.

$$OP=\frac{b_A}{\sqrt{M_A}}\exp\{-W_A\}\mathbf{K}\,.\,\mathbf{P},$$

$$PR=\frac{b_B}{\sqrt{M_B}}\exp\{-W_B\}\mathbf{K}\,.\,\mathbf{R},$$

$$OP'=\frac{b_A}{\sqrt{M_A}}\exp\{-W_A\}\mathbf{K}'\,.\,\mathbf{P},$$

$$P'R'=\frac{b_B}{\sqrt{M_B}}\exp\{-W_B\}\mathbf{K}'\,.\,\mathbf{R};$$

$$X\hat{O}P=\mathbf{H}\,.\,\mathbf{x}^0(A),\quad X'\hat{P}R=X'\hat{P}'R'=\mathbf{H}\,.\,\mathbf{x}^0(B);$$
$$|F(\mathbf{H},\mathbf{q})|\neq|F(\mathbf{H},\bar{\mathbf{q}})|.$$

(*c*) *Coherent one-phonon process: anomalous scattering*

The presence of anomalous scattering causes an intensity difference at the points defined by $\mathbf{K}$ and $\bar{\mathbf{K}}$ on the scattering surface. Fig. 5 gives the Argand diagram for the one-phonon process where atom *B* is an anomalous scatterer. The elliptic motion of the atom *B* gives rise to two scattering lengths for coherent inelastic scattering as represented by *QR* and *RS* in the Figure. Associated with each of these scattering lengths there will be a component due to anomalous scattering ahead in phase by $\pi/2$. Thus, in the Argand diagram, SR'' and $R''S''$ are the two anomalous scattering lengths associated with *QR* and *RS* respectively. From the diagram one sees that up to the point *S*, there is symmetry between $\mathbf{K}$ and $\bar{\mathbf{K}}$ reflexions. For the reflexion $\mathbf{K}$, the components *RS* and SR'' add as they are in the same phase whereas for $\bar{\mathbf{K}}$, the component *RS* is subtracted from $S\bar{R}''$ as they are in opposite phases. A similar asymmetry occurs for the component $R''S''$ also. That is $|F(\mathbf{K})\neq|F(\bar{\mathbf{K}})|$. The expressions for the intensity at $\mathbf{K}$ and $\bar{\mathbf{K}}$ on the scattering surface can be written down from the Argand diagram. Apart from a constant factor, we have

$$I(\mathbf{K})=\frac{b_A^2}{M_A}\exp\{-2W_A\}\{(\mathbf{K}\cdot\mathbf{P})^2+(\mathbf{K}\cdot\mathbf{Q})^2\}$$
$$+\frac{\exp\{-2W_B\}}{M_B}[\{(b_{B_0}+b'_B)\mathbf{K}\cdot\mathbf{R}-b''_B\mathbf{K}\cdot\mathbf{S}\}^2$$
$$+\{(b_{B_0}+b'_B)\mathbf{K}\cdot\mathbf{S}+b''_B\mathbf{K}\cdot\mathbf{R}\}^2]$$
$$+\frac{2\exp\{-(W_A+W_B)\}}{\sqrt{M_AM_B}}$$
$$\times[b_A\{(b_{B_0}+b'_B)\mathbf{K}\cdot\mathbf{R}-b''_B\mathbf{K}\cdot\mathbf{S}\}$$
$$\times\{\mathbf{K}\cdot\mathbf{P}\cos\mathbf{H}\cdot\mathbf{x}^0(B)-\mathbf{x}^0(A)$$
$$+\mathbf{K}\cdot\mathbf{Q}\sin\mathbf{H}\cdot\mathbf{x}^0(B)-\mathbf{x}^0(A)\}$$
$$-b_A\{(b_{B_0}+b'_B)\mathbf{K}\cdot\mathbf{S}+b''_B\mathbf{K}\cdot\mathbf{R}\}$$

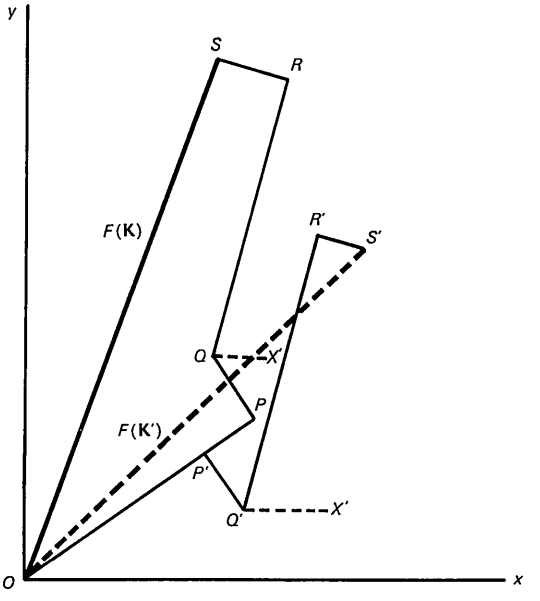

Fig. 9. One-phonon absorption and emission processes near a reciprocal lattice point – eigenvectors complex.

$$OP=\frac{b_A}{\sqrt{M_A}}\exp\{-W_A\}\mathbf{K}\cdot\mathbf{P},$$
$$OP'=\frac{b_A}{\sqrt{M_A}}\exp\{-W_A\}\mathbf{K}'\cdot\mathbf{P},$$
$$PQ=\frac{b_A}{\sqrt{M_A}}\exp\{-W_A\}\mathbf{K}\cdot\mathbf{Q},$$
$$P'Q'=\frac{b_A}{\sqrt{M_A}}\exp\{-W_A\}\mathbf{K}'\cdot\mathbf{Q},$$
$$QR=\frac{b_B}{\sqrt{M_B}}\exp\{-W_B\}\mathbf{K}\cdot\mathbf{R},$$
$$Q'R'=\frac{b_B}{\sqrt{M_B}}\exp\{-W_B\}\mathbf{K}'\cdot\mathbf{R},$$
$$RS=\frac{b_B}{\sqrt{M_B}}\exp\{-W_B\}\mathbf{K}\cdot\mathbf{S},$$
$$R'S'=\frac{b_B}{\sqrt{M_B}}\exp\{-W_B\}\mathbf{K}'\cdot\mathbf{S};$$
$$X\hat{O}P=\mathbf{H}\cdot\mathbf{x}^0(A),\quad X'\hat{Q}R=X'\hat{Q}'R'=\mathbf{H}\cdot\mathbf{x}^0(B);$$
$$|F(\mathbf{H},\mathbf{q})|\neq|F(\mathbf{H},\bar{\mathbf{q}})|.$$

$$\times\{\mathbf{K}\cdot\mathbf{P}\sin\mathbf{H}\cdot\mathbf{x}^0(B)-\mathbf{x}^0(A)$$
$$-\mathbf{K}\cdot\mathbf{Q}\cos\mathbf{H}\cdot\mathbf{x}^0(B)-\mathbf{x}^0(A)\},$$
$$\Delta I=I(\bar{\mathbf{K}})-I(\mathbf{K})=\frac{4\exp\{-(W_A+W_B)\}}{\sqrt{M_AM_B}}$$
$$\times b_Ab''_B[\mathbf{K}\cdot\mathbf{R}\{\mathbf{K}\cdot\mathbf{P}\sin\mathbf{H}\cdot\mathbf{x}^0(B)-\mathbf{x}^0(A)$$
$$-\mathbf{K}\cdot\mathbf{Q}\cos\mathbf{H}\cdot\mathbf{x}^0(B)-\mathbf{x}^0(A)\}$$
$$\times\mathbf{K}\cdot\mathbf{S}\{\mathbf{K}\cdot\mathbf{P}\cos\mathbf{H}\cdot\mathbf{x}^0(B)-\mathbf{x}^0(A)$$
$$+\mathbf{K}\cdot\mathbf{Q}\sin\mathbf{H}\cdot\mathbf{x}^0(B)-\mathbf{x}^0(A)\}].$$

Choosing a second wavelength for the incident thermal neutrons so that the dispersion terms b'_B and b''_B are altered and repeating the experiment at $\mathbf{K}$ and $\bar{\mathbf{K}}$, we get two more independent equations. This is true only if the value of $b''_B/(b_{B_0}+b'_B)$ is not the same for the two wavelengths. From these four independent equations, the unknowns $\mathbf{K}\cdot\mathbf{P}$, $\mathbf{K}\cdot\mathbf{Q}$, $\mathbf{K}\cdot\mathbf{R}$ and $\mathbf{K}\cdot\mathbf{S}$ can be found. Now we consider the inelastic scattering near other reciprocal-lattice points corresponding to the interaction with the same phonon (*i.e.* phonon of same energy and $\mathbf{q}$). Repeating the experiment for two different scattering vectors, we obtain twelve independent equations from which all the components of $\mathbf{P}$, $\mathbf{Q}$, $\mathbf{R}$ and $\mathbf{S}$ can be extracted. Thus the determination of the real and imaginary components of an eigenvector is equivalent to solving the 'phase problem' associated with the initial phase of the elliptic motion.

(*d*) *Interaction with an optical phonon*

For the optical phonon with $\mathbf{q}=0$, the initial phase difference between the two atoms is π. The eigenvectors are real for this mode for all crystal structures. Fig. 6 gives the relevant Argand diagram. The expressions for the intensity at $\mathbf{K}$ and $\bar{\mathbf{K}}$ get considerably simplified if the eigenvectors are real. From Fig. 6,

$$I(\mathbf{K})=\frac{b_A^2}{M_A}\exp\{-2W_A\}(\mathbf{K}\cdot\mathbf{P})^2$$
$$+\frac{\exp\{-2W_B\}}{M_B}\{(b_{B_0}+b'_B)^2+(b''_B)^2\}(\mathbf{K}\cdot\mathbf{R})^2$$
$$+2\frac{\exp\{-(W_A+W_B)\}}{\sqrt{M_AM_B}}b_A(b_{B_0}+b'_B)$$
$$\times\mathbf{K}\cdot\mathbf{R}\,\mathbf{K}\cdot\mathbf{P}\cos\mathbf{H}\cdot\mathbf{x}^0(B)-\mathbf{x}^0(A)$$
$$-2\frac{\exp\{-(W_A+W_B)\}}{\sqrt{M_AM_B}}b_Ab''_B$$
$$\times\mathbf{K}\cdot\mathbf{R}\,\mathbf{K}\cdot\mathbf{P}\sin\mathbf{H}\cdot\mathbf{x}^0(B)-\mathbf{x}^0(A),$$
$$\Delta I=I(\bar{\mathbf{K}})-I(\mathbf{K})=4\frac{\exp\{-(W_A+W_B)\}}{\sqrt{M_AM_B}}$$
$$\times b_Ab''_B\,\mathbf{K}\cdot\mathbf{P}\,\mathbf{K}\cdot\mathbf{R}\sin\mathbf{H}\cdot\mathbf{x}^0(B)-\mathbf{x}^0(A).$$

Since $\mathbf{K}\cdot\mathbf{P}$ and $\mathbf{K}\cdot\mathbf{R}$ are the only two unknowns, measurement at one wavelength determines them. Choosing two different scattering vectors and considering the interaction with the same phonon, the six

components characterizing the vectors **P** and **R** can be extracted. Thus, in cases, where the vibrations are linearly polarized (real eigenvectors) expressions for I and ΔI get considerably simplified and only six measurements are required to characterize the polarization vector.

(*e*) *Coherent one-phonon absorption and emission processes near a reciprocal lattice point*

(i) *Eigenvectors real*

The phonon creation and annihilation processes near a reciprocal lattice point defined by **H** are characterized by the conservation laws,

$$\mathbf{K} = \mathbf{k} - \mathbf{k}_0 = \mathbf{q} + \mathbf{H}$$
$$\mathbf{K}' = \mathbf{k}' - \mathbf{k}_0 = \tilde{\mathbf{q}} + \mathbf{H}.$$

A schematic diagram expressing these momentum conservation laws is given in Fig. 7(*a*). It is clear from the diagram that the scattering vectors corresponding to phonon creation and annihilation processes, are different. That is $|\mathbf{K}|$ is different from $|\mathbf{K}'|$ and differently oriented with respect to the eigenvectors so that the cross sections at the points **K** and **K**′ on the scattering surface are different.

The intensity for **K** and **K**′ reflexions (see Fig. 8) are given by the equations

$$I(\mathbf{K}) = \frac{b_A^2}{M_A} \exp\{-2W_A\} (\mathbf{K} \cdot \mathbf{P})^2 + \frac{b_B^2}{M_B} \exp\{-2W_B\} (\mathbf{K} \cdot \mathbf{R})^2 + 2 \frac{b_A b_B}{\sqrt{M_A M_B}} \exp\{-(W_A + W_B)\} \times \mathbf{K} \cdot \mathbf{P}\, \mathbf{K} \cdot \mathbf{R} \cos \mathbf{H} \cdot \mathbf{x}^0(B) - \mathbf{x}^0(A),$$

$$I(\mathbf{K}') = \frac{b_A^2}{M_A} \exp\{-2W_A\} (\mathbf{K}' \cdot \mathbf{P})^2 + \frac{b_B^2}{M_B} \exp\{-2W_B\} (\mathbf{K}' \cdot \mathbf{R})^2 + 2 \frac{b_A b_B}{\sqrt{M_A M_B}} \exp\{-(W_A + W_B)\} \times \mathbf{K}' \cdot \mathbf{P}\, \mathbf{K}' \cdot \mathbf{R} \cos \mathbf{H} \cdot \mathbf{x}^0(B) - \mathbf{x}^0(A).$$

Making use of the momentum conservation laws, we get

$$\Delta I = I(\mathbf{K}) - I(\mathbf{K}') = 4 \frac{b_A^2 \exp\{-2W_A\}}{M_A} \mathbf{q} \cdot \mathbf{P}\, \mathbf{H} \cdot \mathbf{P} + 4 \frac{b_B^2 \exp\{-2W_B\}}{M_B} \mathbf{q} \cdot \mathbf{R}\, \mathbf{H} \cdot \mathbf{R} + 4 \frac{b_A b_B \exp\{-(W_A + W_B)\}}{\sqrt{M_A M_B}} \times \{\mathbf{H} \cdot \mathbf{P} \mathbf{q} \cdot \mathbf{R} + \mathbf{q} \cdot \mathbf{P}\, \mathbf{H} \cdot \mathbf{R}\} \cos \mathbf{H} \cdot \mathbf{x}^0(B) - \mathbf{x}^0(A).$$

$\Delta I = 0$ only when $\mathbf{H} \cdot \mathbf{P} = \mathbf{H} \cdot \mathbf{R} = 0$ or $\mathbf{q} \cdot \mathbf{P} = \mathbf{q} \cdot \mathbf{R} = 0$.

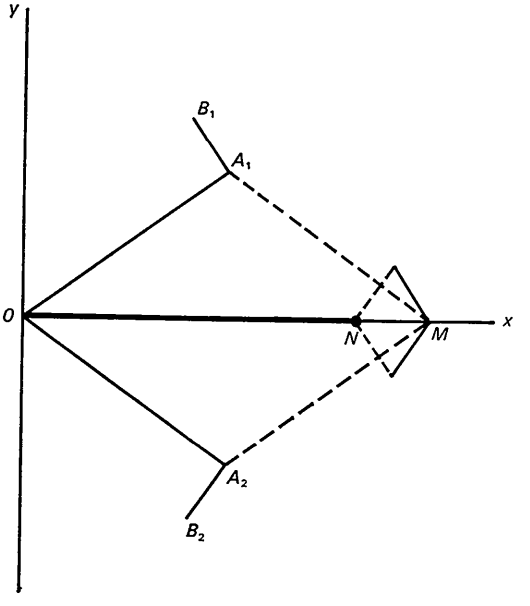

Fig. 10. One-phonon scattering in a centrosymmetric structure – normal scattering.

$$OA_1 = OA_2 = \frac{b}{\sqrt{M}} \exp\{-W\} \mathbf{K} \cdot \mathbf{A},$$
$$A_1B_1 = A_2B_2 = \frac{b}{\sqrt{M}} \exp\{-W\} \mathbf{K} \cdot \mathbf{B},$$
$$OM = \frac{2b}{\sqrt{M}} \exp\{-W\} \mathbf{K} \cdot \mathbf{A} \cos \mathbf{H} \cdot \mathbf{x},$$
$$MN = \frac{2b}{\sqrt{M}} \exp\{-W\} \mathbf{K} \cdot \mathbf{B} \sin \mathbf{H} \cdot \mathbf{x}.$$

Table 1. *Components of the polarization vector and the mode of extracting them by anomalous neutron scattering*

Number	Structure	Number of atoms per unit cell	Number of components of the polarization vector	Number of wavelengths to be used for the thermal neutrons	Number of scattering vectors for which experiments are to be performed
1	Non-centrosymmetric	2	(*a*) 12 (elliptic polarization)	2	3
			(*b*) 6 (linear polarization)	1	3
2	Centrosymmetric	2	(*a*) 6 (elliptic polarization)	2	3
			(*b*) 3 (linear polarization)	1	3
3	Bravais lattice	1	3	1	3

This condition corresponds to a highly symmetric case when the lattice wave is propagating normal to **H**. Then the intensity at the two points defined by **K** and **K′** is equal. This special case is given in Fig. 7(*b*). Thus one gets the result that even in rock salt-type structures where the eigenvectors are always real, the intensity for **K** and **K′** on the scattering surface should be different.

(ii) *Eigen-vectors complex*

When the eigenvectors are complex signifying elliptic motions, we have the following relations

$$\mathbf{e}(A|\mathbf{q}_j)=\mathbf{e}^*(A|\bar{\mathbf{q}}_j)=\mathbf{P}+i\mathbf{Q}$$
$$\text{and } \mathbf{e}(B|\mathbf{q}_j)=\mathbf{e}^*(B|\bar{\mathbf{q}}_j)=\mathbf{R}+i\mathbf{S}\,.$$

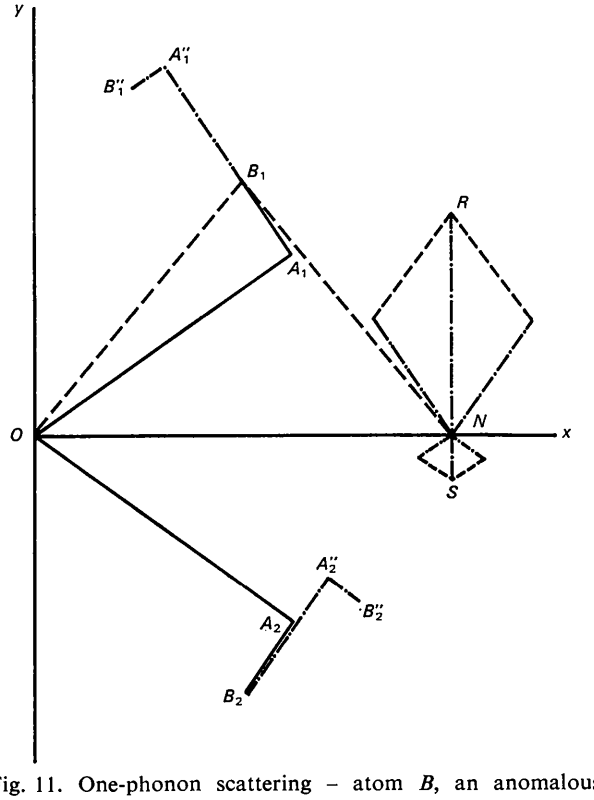

Fig. 11. One-phonon scattering – atom *B*, an anomalous scatterer.

$$B_1A_1''=B_2A_2''=\frac{b''}{\sqrt{M}}\exp\{-W\}\mathbf{K}\,.\,\mathbf{A},$$

$$A_1''B_1''=A_2''B_2''=\frac{b''}{\sqrt{M}}\exp\{-W\}\mathbf{K}\,.\,\mathbf{B},$$

$$ON=2\,\frac{(b_0+b')}{\sqrt{M}}\exp\{-W\}$$
$$\times[\mathbf{K}\,.\,\mathbf{A}\cos\mathbf{H}\,.\,\mathbf{x}-\mathbf{K}\,.\,\mathbf{B}\sin\mathbf{H}\,.\,\mathbf{x}],$$

$$NR=2\,\frac{b''}{\sqrt{M}}\exp\{-W\}\mathbf{K}\,.\,\mathbf{A}\cos\mathbf{H}\,.\,\mathbf{x},$$

$$NS=2\,\frac{b''}{\sqrt{M}}\exp\{-W\}\mathbf{K}\,.\,\mathbf{B}\sin\mathbf{H}\,.\,\mathbf{x};$$

$$|F(\mathbf{K})|=|F(\bar{\mathbf{K}})|.$$

Thus for the phonon absorption process, the imaginary component **K** . **Q** leads the real component **K** . **P** in phase by $\pi/2$ while for the emission process **K′** . **Q** lags **K′** . **P** in phase by $\pi/2$. Then the intensity difference between **K** and **K′** reflexions arises from two causes. Firstly, the scattering vectors for the two processes are different and hence the cross sections are different. There is a further intensity difference, owing to the elliptic motions of the atoms. Fig. 9 represents the Argand diagram for phonon absorption and creation processes when both the atoms in the structure are describing elliptic motions.

As noted earlier, determination of the polarization vector requires measurements to be made for three different scattering vectors. Since the phonon absorption and emission processes around a reciprocal-lattice point correspond to two different scattering vectors, measurements around two reciprocal-lattice points, are sufficient for the determination of the polarization vector.

5. Centro-symmetric structures

(*a*) *Coherent one-phonon process: normal scattering*

Consider a centrosymmetric structure with two atoms per unit cell, where the centre of inversion does not coincide with the atomic positions. Under the influence of a lattice wave, except in symmetry directions, the two atoms describe motion along identical ellipses but in opposite sense. That is, the eigenvectors for the two centrosymmetrically-related atoms, are complex conjugates of one another.

$$\mathbf{e}(\kappa|\mathbf{q}_j)=\mathbf{e}^*(\bar{\kappa}|\mathbf{q}_j)$$

where κ and $\bar{\kappa}$ are the two centrosymmetrically related atoms in the unit cell. Let **x** and $\bar{\mathbf{x}}$ denote the equilibrium position vectors of these two atoms. We write

$$\mathbf{e}(\kappa|\mathbf{q}_j)=\mathbf{A}+i\mathbf{B}\,.$$

Fig. 10 represents the Argand diagram for coherent one phonon process in a centrosymmetric structure when both the atoms are normal scatterers for neutrons. The scattering lengths $(b/\sqrt{M})\exp\{-W\}\mathbf{K}\,.\,\mathbf{A}$ corresponding to the real part of the eigenvector can be added for κ and $\bar{\kappa}$ atoms, to give the resultant scattering length OM along the real axis. The components $(b/\sqrt{M})\exp\{-W\}\mathbf{K}\,.\,\mathbf{B}$ which arise owing to ellipticity can again be added for κ and $\bar{\kappa}$ atoms to give the resultant MN along the real axis which is opposite in phase with respect to OM. Further the same diagram holds good for the reflexion $\bar{\mathbf{K}}$ also, because $\mathbf{K}\,.\,\mathbf{x}=\bar{\mathbf{K}}\,.\,\bar{\mathbf{x}}$ and $\mathbf{K}\,.\,\bar{\mathbf{x}}=\bar{\mathbf{K}}\,.\,\mathbf{x}$ and $|\mathbf{K}|=|\bar{\mathbf{K}}|$. That is $|F(\mathbf{K})|=|F(\bar{\mathbf{K}})|$

$$I(\mathbf{K})=I(\bar{\mathbf{K}})=\frac{4b^2}{M}\exp\{-2W\}\,[\mathbf{K}\,.\,\mathbf{A}\cos\mathbf{H}\,.\,\mathbf{x}$$
$$-\mathbf{K}\,.\,\mathbf{B}\sin\mathbf{H}\,.\,\mathbf{x}]^2$$

where b represents the normal scattering length of the atom.

(b) Coherent one-phonon process: anomalous scattering

The ellipses characterizing the motions of the two atoms being identical, only six components are required to characterize the polarization vector. For the reflexion **K** associated with the phonon wave-vector **q**, one has to add the contributions of both the centrosymmetrically related atoms. This leads to perfect symmetry between **K** and $\bar{\mathbf{K}}$ reflexions, so that the intensities at these two points on the scattering surface are equal even for anomalous scattering. Fig. 11 gives the Argand diagram for a centrosymmetric structure in the presence of anomalous scattering. The various scattering lengths for κ and $\bar{\kappa}$ atoms can be added so as to give a scattering length along the real axis and another component along the imaginary axis. From Fig. 11,

$$I(\mathbf{K})=I(\bar{\mathbf{K}})=4\frac{(b_0+b')^2}{M}\exp\{-2W\}\times\{\mathbf{K}\,.\,\mathbf{A}\cos\mathbf{H}\,.\,\mathbf{x}-\mathbf{K}\,.\,\mathbf{B}\sin\mathbf{H}\,.\,\mathbf{x}\}^2+4\frac{(b'')^2}{M}\exp\{-2W\}\times\{\mathbf{K}\,.\,\mathbf{A}\cos\mathbf{H}\,.\,\mathbf{x}-\mathbf{K}\,.\,\mathbf{B}\sin\mathbf{H}\,.\,\mathbf{x}\}^2\,.$$

Choosing another wavelength for the incident thermal neutrons so that the dispersion terms b' and b'' are altered and repeating the experiment, we arrive at two independent equations from which **K . A** and **K . B** can be determined. The same procedure is followed for two different scattering vectors corresponding to the interaction with the same phonon. From these six measurements, we can solve for the six components of **A** and **B**.

(c) Coherent one-phonon absorption and emission processes near a reciprocal-lattice point

Fig. 12 gives the Argand diagram representation of the phonon absorption and emission processes near a reciprocal-lattice point. The intensity difference at the points defined by **K** and **K'** is again associated with the change in scattering vectors as well as the ellipticity of the motions of the two atoms. In Fig. 12, ON represents the structure factor $F(\mathbf{K})$ which is obtained by addition of the scattering lengths for the two centrosymmetrically related atoms. Similarly OT represents the structure factor $F(\mathbf{K}')$. From Fig. 12,

$$\Delta I=I(\mathbf{K})-I(\mathbf{K}')=4\frac{b^2\exp\{-2W\}}{M}\times[\{\mathbf{K}\,.\,\mathbf{A}\cos\mathbf{H}\,.\,\mathbf{x}-\mathbf{K}\,.\,\mathbf{B}\sin\mathbf{H}\,.\,\mathbf{x}\}^2-\{\mathbf{K}'\,.\,\mathbf{A}\cos\mathbf{H}\,.\,\mathbf{x}+\mathbf{K}'\,.\,\mathbf{B}\sin\mathbf{H}\,.\,\mathbf{x}\}^2]\,.$$

As in the non-centrosymmetric case, the two scattering vectors corresponding to the phonon absorption and creation processes can be effectively made use of in the determination of the polarization vector.

(d) Bravais Lattice

In the case of a Bravais lattice which has one atom per unit cell, the eigenvector being real, is linearly polarized so that only three components are required to describe the polarization vector. The measurement of intensity for three different scattering vectors is sufficient to characterize the polarization vector. The Argand diagram for the coherent one-phonon scattering in a Bravais lattice is very much simplified as only one real scattering length is involved.

Table 1 summarizes the discussion giving the components of the polarization vector and the mode of extracting them by anomalous neutron scattering.

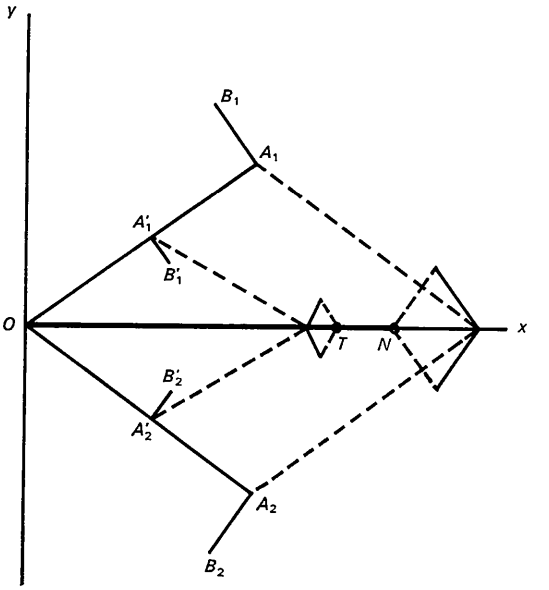

Fig. 12. One-phonon absorption and emission processes near a reciprocal-lattice point – centrosymmetric structure; eigenvectors complex.

$$OA_1=OA_2=\frac{b}{\sqrt{M}}\exp\{-W\}\mathbf{K}\,.\,\mathbf{A},$$

$$OA_1'=OA_2'=\frac{b}{\sqrt{M}}\exp\{-W\}\mathbf{K}'\,.\,\mathbf{A},$$

$$A_1B_1=A_2B_2=\frac{b}{\sqrt{M}}\exp\{-W\}\mathbf{K}\,.\,\mathbf{B},$$

$$A_1'B_1'=A_2'B_2'=\frac{b}{\sqrt{M}}\exp\{-W\}\mathbf{K}'\,.\,\mathbf{B},$$

$$ON=2\frac{b}{\sqrt{M}}\exp\{-W\}\times[\mathbf{K}\,.\,\mathbf{A}\cos\mathbf{H}\,.\,\mathbf{x}-\mathbf{K}\,.\,\mathbf{B}\sin\mathbf{H}\,.\,\mathbf{x}],$$

$$OT=2\frac{b}{\sqrt{M}}\exp\{-W\}\times[\mathbf{K}'\,.\,\mathbf{A}\cos\mathbf{H}\,.\,\mathbf{x}+\mathbf{K}'\,.\,\mathbf{B}\sin\mathbf{H}\,.\,\mathbf{x}].$$

Conclusion

The determination of the polarization vectors seems to involve a number of experimental problems (see for example, Dolling & Woods, 1965; Brockhouse, 1964). The recent evaluation of the polarization vector of the ferroelectric soft mode in KD_2PO_4 by Skalyo, Frayer & Shirane (1970) is of some interest in this connexion. It is not possible to foresee all the obstacles that may be encountered when the anomalous scattering technique as proposed in this paper is used for determining the polarization vectors. It may be necessary to use lower concentrations of the anomalously scattering isotope in the specimen. However, in view of the inherent directness of this method, it appears worth while pursuing this experimental approach.

The authors wish to thank Mr Rajaram Nityananda for the discussions they had with him.

References

BROCKHOUSE, B. N. (1964). *Phonons and Phonon Interactions*, pp. 221–275. New York: Benjamin.
COCHRAN, W. (1968), *Neutron Inelastic Scattering*, Vol. I, pp. 275–280. Vienna: IAEA. SM-104/121.
DOLLING, G. & WOODS, A. D. B. (1965). *Thermal Neutron Scattering*, pp. 193–249. London: Academic Press.
MARADUDIN, A. A., MONTROLL, E. W. & WEISS, G. H. (1963). *Theory of Lattice Dynamics in the Harmonic Approximation*. New York: Academic Press.
PETERSON, S. W. & SMITH, H. G. (1961). *Phys. Rev. Letters*, **6**, 7.
PETERSON, S. W. & SMITH, H. G. (1962). *J. Phys. Soc. Japan*, **17**, 335.
RAMASESHAN, S. (1966). *Curr. Sci.* **35**, 87.
RAMASESHAN, S. & VISWANATHAN, K. S. (1970). *Acta Cryst.* A**26**, 364.
SINGH, A. K. & RAMASESHAN, S. (1968). *Acta Cryst.* B**24**, 35.
SKALYO, J. JR, FRAZER, B. C. & SHIRANE (1970). *Phys. Rev.* B**1**, 278.

Acta Cryst. (1971). A**27**, 341

The Performances of Neutron Collimators
I. Accurate Transmitted Intensity Evaluations for Neutron Collimator Systems

BY F. ROSSITTO
CESNEF, Politecnico di Milano, Milan, Italy

AND G. POLETTI
Gruppo Struttura della Materia, CISE, Milan, Italy

(*Received* 2 *October* 1970)

Limitations imposed by the geometry of Soller collimator systems on luminosity and resolution of neutron diffraction equipment are studied on the grounds of angular and spatial distribution of neutrons. Transmission functions for collimator systems of arbitrary complexity are derived. The influence of the mutual distances among the various components of the experimental set-up on the shape of transmission functions is given in evidence. Careful intensity measurements performed with well diversified arrangements of Soller collimators are in fair agreement with our theoretical results. The way to improve the performances of neutron diffraction equipment by a proper choice of all the geometrical parameters is shown.

1. Introduction

The influence of collimator parameters (typically the angular divergence) on luminosity and resolution of single or multi-axis neutron spectrometers is usually derived on the basis of Sailor's hypothesis (Sailor, Foote, Landon & Wood, 1956; Caglioti, Paoletti & Ricci, 1958, 1960; Caglioti & Ricci, 1962; Popovici & Gelberg, 1966). Sailor *et al.* (1956) assume that collimator transmission functions can be conveniently described by a Gaussian function $n(\varphi)$, where φ is the angle between the projection of any individual neutron trajectory on a horizontal plane and the collimator centre line; the full width at half maximum of the Gaussian distribution is the angular divergence of the collimator.

Nevertheless neutron sources and collimators are quite sizeable, so that a more correct approach should take into account the dependence of transmission functions not only on direction but also on position of any individual neutron. In this last way Szabó (1959) and Jones (1962) worked out relations on intensity and parameter optimization limited to a single (primary) collimator, and Carpenter (1963) discussed a more general approach to the problem, giving a graphical representation of collimator transmission functions.

In the following sections we derive general transmission functions for neutron collimator systems, taking